Journal of Food Measurement and Characterization (2023) 17:5821–5827
https://doi.org/10.1007/s11694-023-02095-0

ORIGINAL PAPER

Rapid determination of quercetin and caffeic acid in honeysuckle tea by high efficiency electrochemical sensor

Liwen Dou[1] · Hui Han[1] · Binbin Yang[1] · Cuixia Lin[1] · Shaobin Pan[1] · Qingjun Li[1] · Peizheng Yan[1] · Dongsheng Zhao[1] · Xianbing Chang[1] · Jia Li[1]

Received: 31 May 2023 / Accepted: 26 July 2023 / Published online: 3 August 2023

Abstract
This research elucidates the enhanced electrochemical performance of a sensor, utilizing multi-walled carbon nanotubes (MWCNT) modified with Au and 2,6-dioctadecylaminopyridine (DODMA) for the detection of quercetin and caffeic acid. The study highlights the importance of electrode modifications, indicating that MWCNT-Au and DODMA noticeably boost the sensor's electroactivity. For quercetin detection, an optimal pH of 4, an enrichment potential of 0.28 V, and an enrichment time of 15 min were established. For caffeic acid, the sensor showed optimum performance at pH 2.20. Moreover, the sensor demonstrated excellent linearity within two distinct ranges of caffeic acid concentration (0.005-5 μM and 6–50 μM). The DPV method showed recovery rates ranging from 98.20 to 102.42% for quercetin and 99.51–99.82% for caffeic acid in honeysuckle tea, underscoring the sensor's precision and reliability. The promising results of this study show potential applications for this sensor platform in the detection of other bioactive compounds.

Keywords Electrochemical sensor · Honeysuckle · DODMA · Quercetin · Caffeic acid

Introduction

The science of nutraceuticals, functional foods, and herbal supplements has been rapidly evolving with advancements in analytical techniques and the discovery of bioactive compounds. One such herbal concoction that has caught the attention of the scientific community is honeysuckle tea, a traditional drink with rich phytochemical composition, known for its health-promoting properties [1, 2]. Among the plethora of bioactive compounds present in honeysuckle tea, quercetin and caffeic acid have been identified as key elements contributing to its health benefits [3–5]. Quercetin, a flavonoid found in many fruits, vegetables, leaves, and grains, is known for its antioxidant, anti-inflammatory, and anti-carcinogenic properties [6]. It has also been associated with the prevention of cardiovascular diseases and has potential anti-allergic and antiviral properties [7]. On the other hand, caffeic acid, a hydroxycinnamic acid derivative, exhibits strong antioxidant activity and shows potential in preventing various types of cancers, cardiovascular diseases, and neurodegenerative diseases [8]. Therefore, the accurate and rapid detection of these compounds in honeysuckle tea is of significant interest for quality control and standardization, as well as for understanding the potential health benefits [9, 10].

Until recently, the quantification of quercetin and caffeic acid in honeysuckle tea has been challenging due to the complex matrix of this herbal infusion, which includes other phenolic compounds, sugars, amino acids, and minerals. Traditional analytical methods such as High-Performance Liquid Chromatography (HPLC) [11], Ultraviolet-Visible Spectroscopy (UV-Vis) [12], and Mass Spectrometry (MS) [13] have been employed to quantify these compounds. However, these methods are time-consuming, require sophisticated equipment, extensive sample preparation, and are not ideal for real-time or on-site measurements [14, 15]. Moreover, they can potentially alter the natural composition of the sample, making it difficult to correlate the observed effects with the actual composition of the original tea infusion.

✉ Xianbing Chang
cxb8020@163.com

✉ Jia Li
liytl7172@163.com

[1] Shandong University of Traditional Chinese Medicine, Jinan 250355, Shandong, China

In this context, the development of reliable, accurate, and rapid methods for the determination of quercetin and caffeic acid in honeysuckle tea is a pressing need. Among the emerging techniques, electrochemical sensing has shown promise in food analysis due to its high sensitivity, simplicity, rapidity, and potential for miniaturization and real-time measurements [16–19]. Electrochemical sensors operate based on the redox reactions of analytes on the electrode surface, which generate measurable electrical signals. The sensor's performance can be enhanced by using different types of electrodes and modifying the electrode surface with nanomaterials, polymers, or biomolecules [20–24]. Thus, the design of a high-efficiency electrochemical sensor for the detection of quercetin and caffeic acid in honeysuckle tea could address the limitations of traditional methods and contribute significantly to the field of food analysis and quality control.

This study aims to present a novel method for the rapid determination of quercetin and caffeic acid in honeysuckle tea using a high-efficiency electrochemical sensor. We will discuss the design, fabrication, and optimization of the sensor, followed by its validation through comparison with traditional analytical methods. Furthermore, we will explore its potential applications for the on-site and real-time analysis of honeysuckle tea.

The detection and quantification of quercetin and caffeic acid in honeysuckle tea are of significant importance given their health benefits and potential therapeutic applications. A high-efficiency electrochemical sensor can be a game-changer in this context, offering a rapid, accurate, and user-friendly method for the analysis of honeysuckle tea, which can be instrumental for the tea industry, consumers, and researchers. Moreover, the application of high-efficiency electrochemical sensors goes beyond the mere detection of these two crucial phytochemicals. It could catalyze a much-needed revolution in the field of functional food and nutraceutical analysis, ushering in a new era of rapid, cost-effective, and highly sensitive detection methods that could seamlessly integrate into industrial processes and quality control labs.

Experimental

Materials

Dimethyldioctadecylammonium bromide (DODMA), Gold(III) chloride trihydrate (HAuCl4·3H2O), and Polyetherimide (PEI) were procured from Sigma Company. Carboxylic acid functionalized Multi-Walled Carbon nanotube (MWCNT-COOH) was acquired from Nanjing Xianfeng Nanomaterials Technology Co., Ltd. Acetonitrile, ethanol, sodium dihydrogen phosphate, and disodium hydrogen phosphate were purchased from Sinopharm Chemical Reagent Co., Ltd. Caffeic acid and quercetin were obtained from Greensource Biopharmaceutical Co., Ltd.

Preparation of DODMA/MWCNT-Au

An aliquot of 3.4 mg of carboxylic acid functionalized Multi-Walled Carbon Nanotube (MWCNT-COOH) was suspended in 10 mL of ultrapure water and sonicated for 10 min. Then, an excess of Polyetherimide (PEI) was added to the suspension, followed by 5 min of ultrasonic agitation. Subsequently, 2 mL of an 18 mM chloroauric acid (HAuCl4·3H2O) solution was added, and the mixture was reacted at 70 °C for 2 h. The resulting product was washed three times with distilled water using a centrifuge set at 15,000 rpm for 10 min each. The obtained material was then dried completely in a constant temperature blast drying oven and stored at room temperature for future use. A predetermined quantity of MWCNT-Au was suspended in acetonitrile to prepare a 0.3 g/L solution. A 1 g/L solution of Dimethyldioctadecylammonium bromide (DODMA) in ethanol was used as a stock solution and stored at 4 °C. Prior to use, it was diluted to 50 g/L and sonicated until uniform. The glassy carbon electrode (GCE) with a diameter of 3 mm was polished using an alumina solution (0.5 μM) and subsequently cleaned ultrasonically with ethanol and double-distilled water for 2 min. The electrode was then modified by drop-casting 5 μL of the MWCNT-Au solution and 5 μL of the DODMA solution onto the GCE surface, followed by drying under an infrared lamp. The resulting modified electrode is denoted as DODMA/MWCNT-Au/GCE.

Results and discussion

The electrochemical characteristics of each electrode were determined in a 0.1 M KCl solution containing 1 mM $[Fe(CN)_6]^{3-/4-}$, with the scan rate set at 100 mV/s. Figure 1 A portrays the cyclic voltammograms of GCE, MWCNT-COOH/GCE, MWCNT-Au/GCE, and DODMA/MWCNT-Au/GCE in a 0.1 M KCl solution infused with 1 mM $[Fe(CN)_6]^{3-/4-}$. On the GCE, a prominent redox peak pair emerges. When the electrode is modified with MWCNT-Au, the oxidation peak current notably surges, implying the facilitative role of MWCNT-Au in electron transfer [25]. Moreover, when the MWCNT-Au surface is enveloped with a DODMA film, the oxidation peak current further escalates. The findings suggest that both DODMA and MWCNT-Au enhance the electrochemical performance of the sensor [26].

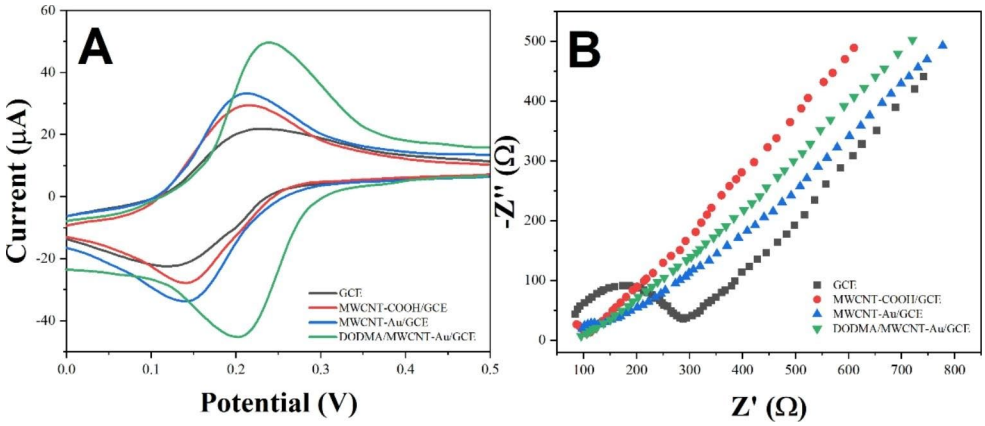

Fig. 1 **(A)** CV and **(B)** EIS plots of GCE, MWCNT-COOH/GCE, MWCNT-Au/GCE, DODMA/MWCNT-Au/GCE in 1 mM $[Fe(CN)_6]^{3-/4-}$ + 0.1 M KCl.

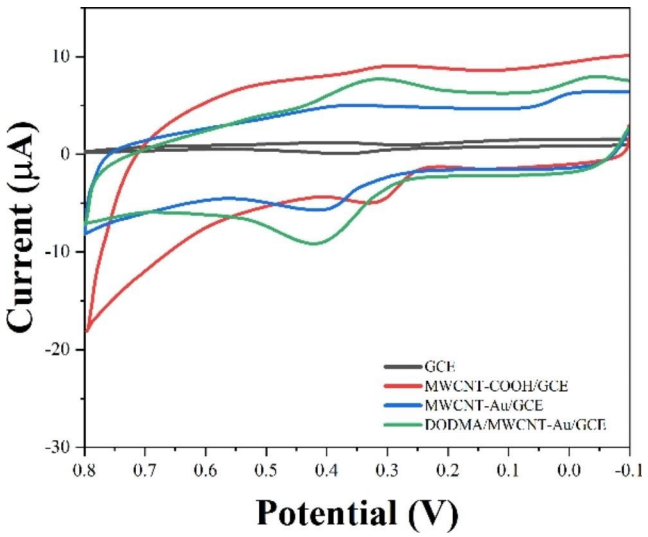

Fig. 2 CVs of GCE, MWCNT-COOH/GCE, MWCNT-Au/GCE, DODMA/MWCNT-Au/GCE towards 0.5 μM quercetin

The EIS spectra of the reaction in a 0.1 M KCl solution containing 5 mM $[Fe(CN)_6]^{3-/4-}$ were also examined for each electrode, as depicted in Fig. 1B. The semicircle diameter representative of charge transfer impedance markedly diminishes for MWCNT-COOH, MWCNT-Au, and DODMA/MWCNT-Au/GCE in comparison with GCE, approaching a straight line, indicating that DODMA/MWCNT-Au possesses superior conductivity, thereby augmenting the charge transfer rate on the GCE surface [27].

The electrochemical behavior of quercetin on various modified GCEs was investigated using CV. As illustrated in Fig. 2, compared with the quercetin oxidation-reduction peak current on bare GCE, the oxidation-reduction peak current of quercetin on MWCNT-COOH-modified GCE significantly increased. This denotes that MWCNT-COOH improved the catalytic activity of quercetin oxidation while simultaneously reducing the effective electrode surface area. The oxidation-reduction peak current of quercetin on MWCNT-Au/GCE markedly exceeded that on MWCNT-COOH/GCE due to the exceptional conductivity of Au clusters amplifying the electrochemical signal [28]. When DODMA was modified onto MWCNT-Au/GCE, an even larger response signal was observed, potentially owing to the excellent supramolecular recognition ability of DODMA molecules, with quercetin as the guest molecule selectively permeating into the cavity of DODMA [29]. Therefore, strong hydrogen bonds form through interactions with hydroxyl groups at the top and bottom of the DODMA cavity. In Fig. 1A, the CV of DODMA/MWCNT-Au/GCE exhibit a shift in the two peaks towards high potential compared to the other electrodes. This observed shift can be attributed to several factors related to the electrochemical behavior of the modified electrode. The presence of MWCNTs and Au clusters in the modification layer significantly affects the electron transfer kinetics on the electrode surface. MWCNTs have a high surface area and excellent electrical conductivity, facilitating electron transfer reactions. The incorporation of Au clusters further enhances the electroactivity of the electrode, amplifying the electrochemical signal. This improved electron transfer efficiency and signal amplification contribute to the observed shift in the peaks towards high potential. The addition of the DODMA film onto the MWCNT-Au-modified electrode also influences the electrochemical behavior. DODMA acts as a supramolecular recognition element, selectively permeating quercetin and forming strong hydrogen bonds with hydroxyl groups of the analyte. The presence of DODMA further enhances the electrochemical performance of the sensor by facilitating the interaction and recognition of quercetin on the electrode surface.

Upon the surface of the modified electrode, the acidity of the buffer solution significantly impacts the electrochemical behavior of quercetin. In this investigation, we studied the effects of a pH range from 3.0 to 6.0 on the electrochemical response of 0.5 μM quercetin on DODMA/MWCNT-Au/GCE using CV. As demonstrated in Fig. 3, the two peak potentials shift negatively with the increase in pH, indicating that protons partake in the electrochemical reaction of quercetin [30]. The linear regression equations for the

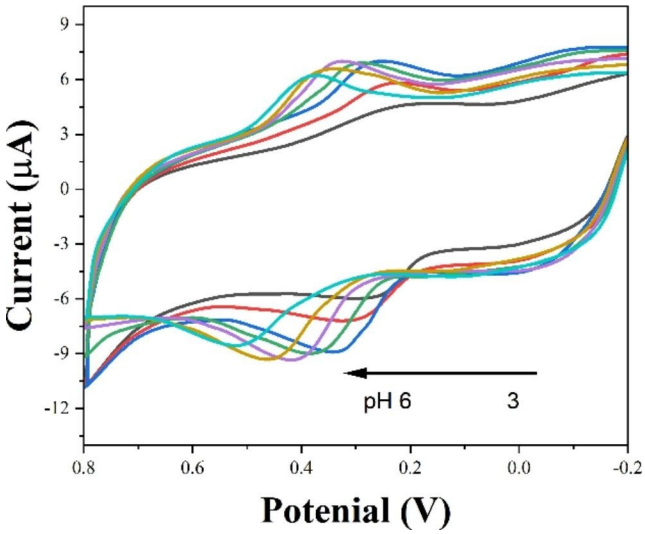

Fig. 3 CVs of DODMA/MWCNT-Au/GCE towards 0.5 μM quercetin with different pH values

reduction process of quercetin in terms of peak potential and pH are E_{pc} (V) = -0.0481pH + 0.4941 (R^2 = 0.9911), and for the oxidation process of quercetin, they are $E_{p.a.}$ (V) = -0.0591pH + 0.6291 (R^2 = 0.9881). In accordance with the Nernst equation, the theoretical value of 0.0591 V/pH is very close to the offset of 0.0580 V/pH, which suggests that in the electro-oxidation reaction of quercetin, the number of transferred electrons and protons is equivalent [31]. Concurrently, the peak current is also influenced by pH. As shown in Fig. 3B, the peak current of quercetin reaches its maximum when the pH level attains 4 and subsequently diminishes.

The observed shift in peak potentials with increasing pH indicates the involvement of protons in the electrochemical reactions of quercetin and caffeic acid. The linear regression equations for the reduction process of quercetin in terms of peak potential and pH and for the oxidation process of quercetin provide insights into the number of transferred electrons and protons involved in the electro-oxidation reaction. The selected optimal pH values were determined based on the observed changes in peak potentials and peak currents.

As depicted in Fig. 4A, the peak current notably amplifies when the quantity of DODMA/MWCNT-Au/GCE elevates from 4.0 to 7.0 μL. However, the peak current slightly declines when the quantity of DODMA/MWCNT-Au/GCE continues to increase from 7.0 to 10.0 μL. The likely explanation is that a thicker DODMA/MWCNT-Au/GCE film hinders electron transfer and impedes the mass transfer process of quercetin [32]. As a result, 7.0 μL of the DODMA/MWCNT-Au composite is utilized as the optimal quantity for modifying GCE throughout the experiment.

Based on the above analysis, the quercetin process on the surface of DODMA/MWCNT-Au/GCE is an adsorption-controlled process. Therefore, to enhance the sensor's detection of quercetin, enrichment potential and enrichment time are two crucial influencing factors worth investigating. As illustrated in Fig. 4B C, the peak current of 0.5 μM quercetin on DODMA/MWCNT-Au/GCE increases within the ranges of -0.28 to 0.28 V for enrichment potential and 1 to 15 min for enrichment time. However, when the enrichment potential exceeds 0.28 V, the peak current sharply declines. Simultaneously, after the enrichment time surpasses 15 min, the oxidation peak current remains nearly unchanged due to the equilibrium state of quercetin adsorption on the electrode material [33]. Hence, the optimal enrichment potential and enrichment time for quercetin measurement are respectively 0.28 V and 15 min.

Predicated upon the aforementioned optimal conditions, the DPV response of 0.005 to 0.5 μM quercetin in 0.10 M HAc-NaAc buffer on DODMA/MWCNT-Au/GCE is depicted in Fig. 5A. It can be observed that as the concentration of quercetin escalates, the peak current gradually increases. Figure 5B showcases a commendable linear relationship between the peak current of quercetin and its concentration, with the linear regression equation being I(μA) = -36.21441 C(μM) + 0.01621 (R^2 = 0.9985), and the detection limit being 0.00177 μM (S/N = 3).

The electrocatalytic oxidation-reduction activity of caffeic acid on bare GCE, MWCNT-COOH/GCE, MWCNT-Au/GCE, DODMA/MWCNT-Au/GCE was investigated using CV. Figure 6 A displays the CV response curves of various modified GCEs in a pH = 2.20 BR buffer solution without caffeic acid, demonstrating no appearance of oxidation-reduction peaks, thus indicating that the blank BR buffer solution does not interfere with the electrochemical detection of caffeic acid on the modified electrode. Mirroring previous findings, DODMA/MWCNT-Au/GCE possesses

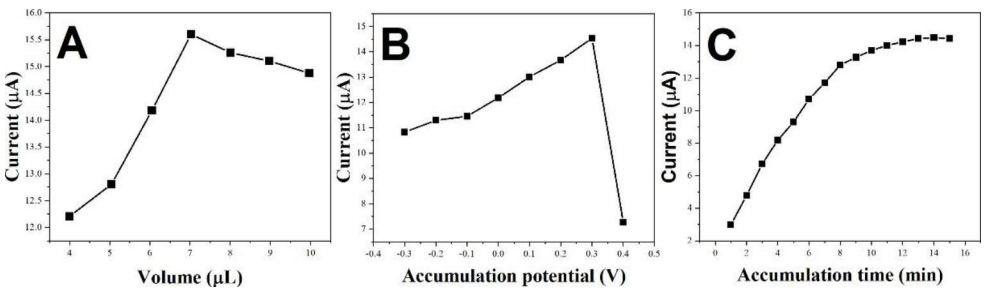

Fig. 4 **(A)** Effect of modified volume of DODMA/MWCNT-Au/GCE on peak current. Relationship between peak current and **(B)** enrichment potential and **(C)** enrichment time

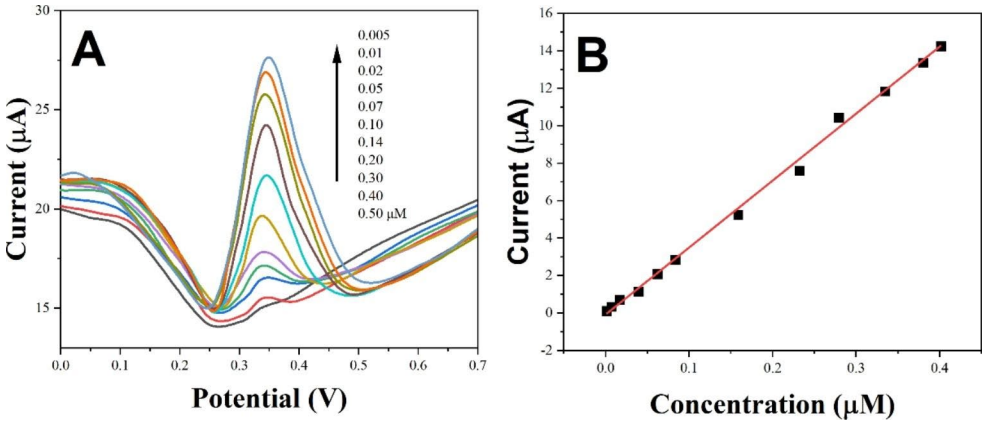

Fig. 5 **(A)** DPV curves of DODMA/MWCNT-Au/GCE toward 0.005, 0.01, 0.02, 0.05, 0.07, 0.10, 0.14, 0.20, 0.30, 0.4 and 0.50 μM quercetin. **(B)** Plots of concentrations and currents

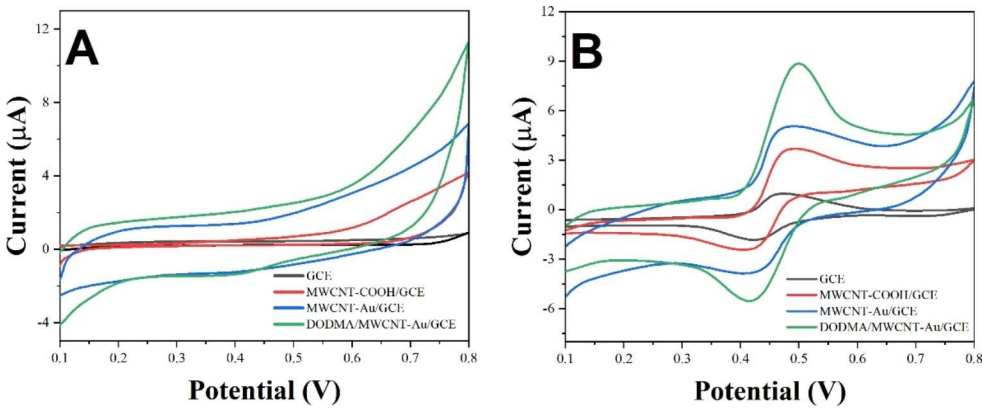

Fig. 6 CV responses of the GCE, MWCNT-COOH/GCE, MWCNT-Au/GCE, DODMA/MWCNT-Au/GCE in the BR solution (pH = 2.20) with the **(A)** absence and **(B)** presence of 40 μM caffeic acid at 50 mV/s

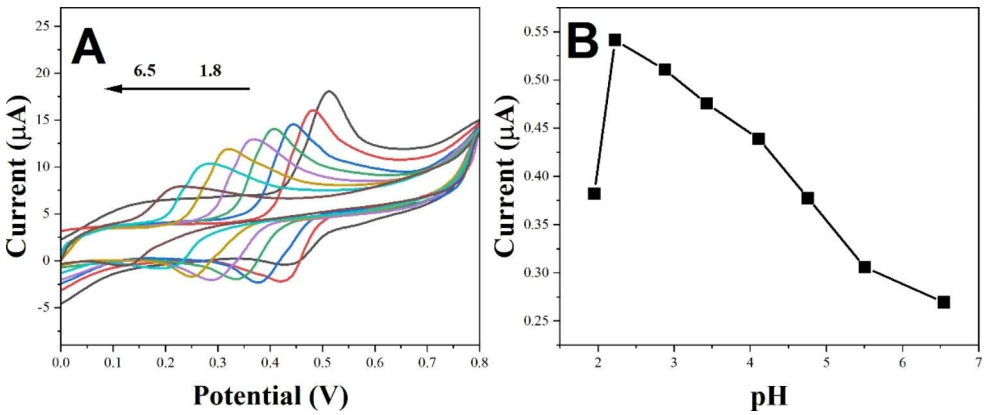

Fig. 7 **(A)** CV responses with different pHs, **(B)** corresponding the plot of Ip/Ep vs. pH) of DODMA/MWCNT-Au/GCE recorded in BR solution (pH = 2.20)

superior electroactivity, favoring the enhancement of caffeic acid's electrochemical sensing performance [34]. Figure 6B exhibits the CV curves of bare GCE, MWCNT-COOH/GCE, MWCNT-Au/GCE, DODMA/MWCNT-Au/GCE in the presence of 40 μM caffeic acid in a pH = 2.20 BR buffer solution. As illustrated, all electrodes possess electro-oxidation-reduction capabilities for caffeic acid, and compared to other electrodes, DODMA/MWCNT-Au/GCE manifests the highest oxidation-reduction peak current, indicating its more prominent electro-oxidation capabilities [35].

The pH value of the electrolyte for the electrochemical oxidation-reduction of caffeic acid was optimized via CV, the results of which are presented in Fig. 7A. As the pH value escalates from 1.92 to 6.50, the oxidation-reduction peak currents first increase and then decrease, reaching their pinnacle when the pH value equals 2.20. Thus, pH = 2.20 is established as the optimal pH value, and all subsequent studies are conducted under this acidity. The oxidation peak potential of caffeic acid shifts in a negative direction, indicating the involvement of protons in this electrochemical reaction process [36]. In addition, the oxidation peak potential ($E_{p.a.}$) is linearly related to pH: Epa = 0.641 + 0.057 pH (Fig. 7B).

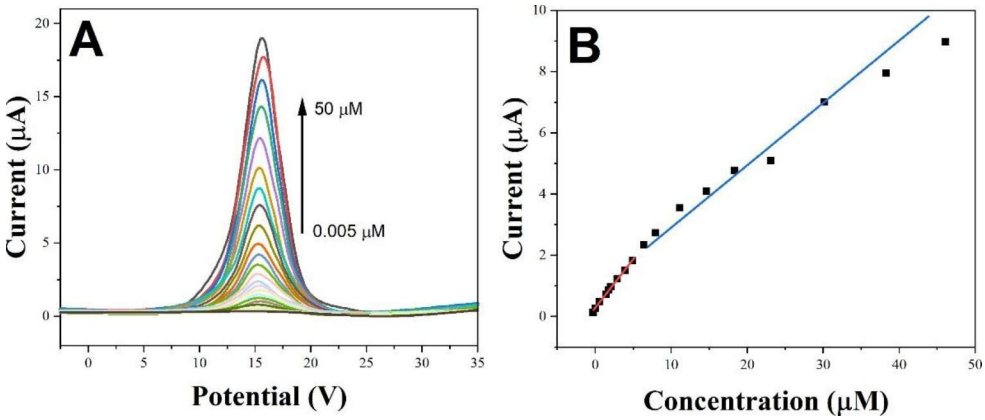

Fig. 8 **(A)** DPV responses of DODMA/MWCNT-Au/GCE in BR solution (pH = 2.20) with various concentrations of caffeic acid from 0.005 to 50 μM. **(B)** Plots of concentrations and currents

Table 1 Detection of quercetin and caffeic acid in honeysuckle tea using proposed DODMA/MWCNT-Au/GCE.

Sample	Detected	Added	Detected	Recovery	RSD
Quercetin					
Honeysuckle tea 1	0.024 μM	0.100 μM	0.125 μM	100.80%	3.41%
Honeysuckle tea 2	0.018 μM	0.200 μM	0.216 μM	99.08%	1.79%
Honeysuckle tea 3	0.034 μM	0.300 μM	0.328 μM	98.20%	2.27%
Caffeic acid					
Honeysuckle tea 1	0.223 μM	1.000 μM	1.217 μM	99.51%	4.05%
Honeysuckle tea 2	0.272 μM	2.000 μM	2.268 μM	99.82%	2.04%
Honeysuckle tea 3	0.191 μM	5.000 μM	5.178 μM	99.75%	3.68%

An analysis employing DPV has been conducted, investigating the electrooxidation reaction of caffeic acid using the DODMA/MWCNT-Au/GCE composite. Figure 8 A illustrates the DPV responses of DODMA/MWCNT-Au/GCE within a caffeic acid concentration range of 0.005-50 μM. As observed in Fig. 8B, the oxidation peak current increases in correlation with the escalating concentrations of caffeic acid. Furthermore, the oxidation peak current demonstrates a linear relationship with caffeic acid concentration within two distinct ranges, 0.005-5 μM and 6–50 μM, as depicted in Fig. 8B. The electrochemical detection limit for caffeic acid using DODMA/MWCNT-Au/GCE is determined to be 2.7 nM (where S/N = 3). These findings suggest that the DODMA/MWCNT-Au/GCE composite material exhibits superior electrochemical sensing capabilities for the oxidation of caffeic acid.

Table 1 showcases the detection of quercetin and caffeic acid in honeysuckle tea using DODMA/MWCNT-Au/GCE. The DPV method reveals recovery rates of 98.20-102.42% for quercetin and 99.51–99.82% for caffeic acid in honeysuckle tea. Thus, the sensor platform designed using DODMA/MWCNT-Au/GCE demonstrates commendable precision and reliability in the DPV detection of quercetin and caffeic acid in genuine beverage samples. This underscores the potential of this platform as a promising sensor.

We examined the electroactivity of the sensor by measuring the CV of the DODMA/MWCNT-Au/GCE over an extended period of time. We observed that the oxidation-reduction peak currents of quercetin and caffeic acid remained relatively stable over the course of several weeks, indicating the sustained electroactivity of the sensor. This stability is attributed to the robustness of the electrode modification, as the DODMA/MWCNT-Au composite provides a stable and conductive surface for the electrochemical reactions. The long-term stability of the sensor ensures consistent and reliable detection of quercetin and caffeic acid in honeysuckle tea.

Furthermore, we assessed the detection capabilities of the sensor after repeated use. We performed multiple measurements of quercetin and caffeic acid in honeysuckle tea using the DPV method. The sensor consistently exhibited excellent linearity and reproducibility within the tested concentration ranges of quercetin and caffeic acid. The recovery rates obtained for quercetin and caffeic acid in honeysuckle tea ranged from 98.20 to 102.42% and 99.51–99.82%, respectively, demonstrating the precision and reliability of the sensor. These results indicate that the sensor maintains its detection capabilities even after repeated use, making it suitable for practical applications in the analysis of honeysuckle tea.

The observed stability and long-term performance of the sensor are crucial for its practical utility and reliability. The sustained electroactivity and detection capabilities of the sensor over time and after repeated use ensure accurate and consistent measurements of quercetin and caffeic acid in honeysuckle tea. These findings highlight the reliability and robustness of the sensor, making it a promising platform for the rapid determination of bioactive compounds not only in honeysuckle tea but also in other applications.

Conclusion

This study successfully demonstrated the enhanced electrochemical performance of a MWCNT-Au and DODMA modified sensor for the detection of quercetin and caffeic acid. The modification of electrodes with MWCNT-Au and DODMA improved the sensor's electroactivity, facilitating increased charge transfer and electron transfer. Additionally, the superior conductivity of MWCNT-Au and DODMA enhanced the sensor's performance. Optimal parameters for quercetin and caffeic acid detection were identified, making the sensor suitable for practical applications. The sensor showed high precision and reliability in detecting quercetin and caffeic acid in honeysuckle tea, with recovery rates ranging from 98.20 to 102.42% for quercetin and 99.51–99.82% for caffeic acid. This research thus provides a promising sensor platform for the detection of other bioactive compounds, paving the way for advancements in the field of electrochemical sensing.

Acknowledgements This work was supported by Demonstration study on large-scale planting of high-quality genuine honeysuckle and targeted poverty alleviation(2017YFC1701503), Youth Innovation Team Support Project for sustainable utilization of traditional Chinese medicine resources of Shandong University of traditional Chinese Medicine, Medical and Health Science and Technology Development Program of Shandong Province (2019WS554).

Declarations

Conflict of interest The authors state that there is no conflict of interest.

References

1. L. Fan, L. Chen, W. Cui, Y. Dong, X. Yuan, L. Wang, J. Liang, S. Zhao, J. Environ. Sci. Health Part B **55**, 921 (2020)
2. Y. Li, W. Ran, C. He, J. Zhou, Y. Chen, Z. Yu, D. Ni, Food Chemistry: X. **14**, 100289 (2022)
3. Y. Gao, Y. Tang, L. Gao, Y. Niu, R. Gao, X. Chen, Y. Hao, S. Wang, Anal. Chim. Acta. **1161**, 338475 (2021)
4. Q. Li, J. Zhang, T. Lin, C. Fan, Y. Li, Z. Zhang, J. Li, Food Res. Int. **166**, 112572 (2023)
5. W. Xie, Y. Yu, M. Hou, Y. Zhang, H. Yu, H. Zhang, G. Zhang, H. Jing, A. Chen, J. Sep. Sci. **45**, 3197 (2022)
6. O. Xiao, M. Li, D. Chen, J. Chen, J. Simal-Gandara, X. Dai, Z. Kong, J. Hazard. Mater. **431**, 128519 (2022)
7. L. Fang, N. Long, Y. Li, X. Liao, L. Shi, H. Zhao, L. Zhou, W. Kong, Ecotoxicol. Environ. Saf. **234**, 113377 (2022)
8. W. Deng, A. Huang, Q. Zheng, L. Yu, X. Li, H. Hu, Y. Xiao, Food Chem. **352**, 129331 (2021)
9. M. Senica, F. Stampar, M.M. PETKOVSEK, Turkish J. Agric. Forestry. **43**, 576 (2019)
10. H. Yang, L. Bao, Y. Liu, S. Luo, F. Zhao, G. Chen, F. Liu, Microchem. J. **171**, 106829 (2021)
11. H. Liu, S. Zhu, Q. Liu, Y. Zhang, Biomed. Chromatogr. **33**, e4583 (2019)
12. S. Wang, C. Mi, L. Wang, Q. Tang, H. Cao, X. Zheng, Int. J. Electrochem. Sci. **17**, 2 (2022)
13. H. Zhou, Y.-M. Cao, S. Miao, L. Lan, M. Chen, W.-T. Li, X.-H. Mao, S. Ji, J. Chromatogr. A **1606**, 460374 (2019)
14. P. Sun, Y. Liu, F. Mo, M. Wu, Y. Xiao, X. Xiao, W. Wang, X. Dong, J. Clean. Prod. **393**, 136320 (2023)
15. P. Sun, L. Cheng, S. Gao, X. Weng, X. Dong, J. Phys. Chem. C **127**, 6610 (2023)
16. H. Shi, L. Fu, F. Chen, S. Zhao, G. Lai, Environ. Res. **209**, 112747 (2022)
17. Y. Xu, Y. Lu, P. Zhang, Y. Wang, Y. Zheng, L. Fu, H. Zhang, C.-T. Lin, A. Yu, Bioelectrochemistry. **133**, 107455 (2020)
18. W. Ye, Y. Zheng, P. Zhang, B. Fan, Y. Li, L. Fu, Int. J. Electrochem. Sci. **16**, 211041 (2021)
19. Y. Zheng, X. Li, F. Han, L. Fu, J. Sun, Int. J. Electrochem. Sci. **16**, 211136 (2021)
20. Y. Liu, W. Zhang, Y. Liu, Int. J. Electrochem. Sci. **18**, 100181 (2023)
21. B. Li, R. Zhang, F. Du, Int. J. Electrochem. Sci. **18**, 100124 (2023)
22. W. Anindya, W.T. Wahyuni, M. Rafi, B.R. Putra, Int. J. Electrochem. Sci. **18**, 100034 (2023)
23. S.I.M. Zayed, A.I. Abdel-Mageed, M.M.A. Majthoub, Int. J. Electrochem. Sci. **18**, 100134 (2023)
24. Q. Li, J.-T. Wu, Y. Liu, X.-M. Qi, H.-G. Jin, C. Yang, J. Liu, G.-L. Li, Q.-G. He, Anal. Chim. Acta. **1170**, 338480 (2021)
25. R. Kaimal, P. Senthilkumar, B. Aljafari, S. Anandan, Analyst. **147**, 3894 (2022)
26. M.A. Chamjangali, A.A. Reskety, N. Goudarzi, G. Bagherian, A.H. Momeni, Biomedical Phys. Eng. Express. **5**, 025029 (2019)
27. Q. Guan, H. Guo, R. Xue, M. Wang, X. Zhao, T. Fan, W. Yang, M. Xu, W. Yang, J. Electroanal. Chem. **880**, 114932 (2021)
28. Y. Rong, M. Jin, Q. Du, Z. Shen, Y. Feng, M. Wang, F. Li, R. Liu, H. Li, C. Chen, J. Mater. Chem. A **10**, 22592 (2022)
29. Y.T. Büyüksünetçi, Ã. Anık, Biosensors. **13**, 176 (2023)
30. M. Alagappan, S. Immanuel, R. Sivasubramanian, A. Kandaswamy, Arab. J. Chem. **13**, 2001 (2020)
31. C.B. Breslin, D. Branagan, L.M. Garry, J. Appl. Electrochem. **49**, 195 (2019)
32. K.S. Galhardo, T.R. Dadamos, R.J.B. da Silva, S.A. Machado, Talanta. **215**, 120883 (2020)
33. T.Ã. Varol, Ã. Anik, New J. Chem. **43**, 13437 (2019)
34. T. Fukuda, H. Muguruma, H. Iwasa, T. Tanaka, A. Hiratsuka, T. Shimizu, K. Tsuji, T. Kishimoto, Anal. Biochem. **590**, 113533 (2020)
35. G. Cho, S. Azzouzi, G. Zucchi, B. Lebental, Sensors. **22**, 218 (2022)
36. S. RoyChoudhury, Y. Umasankar, P. Bhushan, P.A. Hirt, F.E. MacQuhae, L.J. Borda, H.A. Lev-Tov, R. Kirsner, S. Bhansali, J. Electrochem. Soc. **166**, B3295 (2019)